Losartan treatment enhances chemotherapy efficacy and reduces ascites in ovarian cancer models by normalizing the tumor stroma

Yanxia Zhao[a,1], Jinghong Cao[a,2], Alexander Melamed[b,c], Michael Worley[c], Allison Gockley[c], Dennis Jones[a], Hadi T. Nia[a], Yanling Zhang[a], Triantafyllos Stylianopoulos[d], Ashwin S. Kumar[a,e], Fotios Mpekris[d], Meenal Datta[a], Yao Sun[a], Limeng Wu[a,3], Xing Gao[a,3], Oladapo Yeku[b], Marcela G. del Carmen[c], David R. Spriggs[b], Rakesh K. Jain[a,4], and Lei Xu[a,4]

[a]Edwin L. Steele Laboratories, Department of Radiation Oncology, Massachusetts General Hospital, Harvard Medical School, Boston, MA 02114; [b]Gynecologic Cancers Program, Massachusetts General Hospital, Harvard Medical School, Boston, MA 02114; [c]Division of Gynecologic Oncology, Brigham and Women's Hospital, Harvard Medical School, Boston, MA 02130; [d]Cancer Biophysics Laboratory, Department of Mechanical and Manufacturing Engineering, University of Cyprus, 1678 Nicosia, Cyprus; and [e]Harvard–MIT Division of Health Sciences and Technology, Massachusetts Institute of Technology, Cambridge, MA 02139

Contributed by Rakesh K. Jain, December 7, 2018 (sent for review October 26, 2018; reviewed by John Hays and Fan Yuan)

In ovarian cancer patients, tumor fibrosis and angiotensin-driven fibrogenic signaling have been shown to inversely correlate with survival. We sought to enhance drug delivery and therapeutic efficacy by remodeling the dense extracellular matrix in two orthotopic human ovarian carcinoma xenograft models. We hypothesized that targeting the angiotensin signaling axis with losartan, an approved angiotensin system inhibitor, could reduce extracellular matrix content and the associated "solid stress," leading to better anticancer therapeutic effect. We report here four translatable findings: (*i*) losartan treatment enhances the efficacy of paclitaxel—a drug used for ovarian cancer treatment—via normalizing the tumor microenvironment, resulting in improved vessel perfusion and drug delivery; (*ii*) losartan depletes matrix via inducing antifibrotic miRNAs that should be tested as candidate biomarkers of response or resistance to chemotherapy; (*iii*) although losartan therapy alone does not reduce tumor burden, it reduces both the incidence and the amount of ascites formed; and (*iv*) our retrospective analysis revealed that patients receiving angiotensin system inhibitors concurrently with standard treatment for ovarian cancer exhibited 30 mo longer overall survival compared with patients on other antihypertensives. Our findings provide the rationale and supporting data for a clinical trial on combined losartan and chemotherapy in ovarian cancer patients.

ovarian cancer | angiotensin inhibition | drug delivery | ascites | antifibrotic miRNAs

Approximately 22,500 new cases of ovarian cancer are diagnosed annually in the United States, with a mortality of 14,000 (1). Following initial debulking surgery, ovarian cancer patients generally receive a chemotherapy regimen that includes a platinum complex (carboplatin or cisplatin) and a taxane (paclitaxel or docetaxel). However, despite initial responsiveness, the majority of patients with advanced ovarian cancer eventually relapse with resistant disease (2–4). Furthermore, the similarly low response rates for high-grade ovarian cancers to tyrosine kinase inhibitors and immune checkpoint blockers make alternative strategies for ovarian cancer treatment a high clinical priority.

The effective delivery of therapeutic agents to the cancer cells is a primary requirement in successful tumor treatment. To reach cancer cells within a tumor, blood-borne therapeutic agents must be carried by systemic blood flow to the tumor site, cross blood vessel walls, and diffuse through the intervening interstitium (5, 6). We have shown that in highly desmoplastic malignant cancers, such as pancreatic and breast carcinomas, cancer cells, stromal cells, and the fibrotic ECM (i.e., excess deposition of collagen and hyaluronan) contribute to high solid stress (7–11). Solid stress, distinct from fluid pressure, is a physical force contained in and transmitted by the solid phase of the tumor that compresses blood vessels. As tumor blood vessels are structurally abnormal, these vessels are easily collapsible under this high compressive force, resulting in reduced blood flow throughout the tumor mass (8, 9, 11, 12). The reduction in perfusion leads to (*i*) reduced delivery of drugs to tumors, which compromises treatment efficacy (13), and (*ii*) increased tumor hypoxia, which promotes aggressive phenotypes, immunosuppression, and resistance to chemotherapy, radiation, and immunotherapy, which require oxygen to be effective (14).

Significance

Despite initial responsiveness to chemotherapy, the overwhelming majority of advanced ovarian cancer patients relapse with resistant disease. Thus, developing more effective strategies for ovarian cancer treatment is a high clinical priority. Here, we report that targeting angiotensin signaling with losartan, an angiotensin receptor blocker, can reduce extracellular matrix in ovarian tumors and the associated physical barriers that normally hinder drug delivery and efficacy. These changes in the tumor microenvironment lead to improved response to chemotherapy, and, importantly, decrease ascites—a major burden for ovarian cancer patients. These preclinical findings are in concert with our retrospective analysis showing improved survival in patients receiving angiotensin system inhibitors concurrently with standard treatment for ovarian cancer and should be tested in a clinical trial.

Author contributions: Y. Zhao, J.C., D.J., H.T.N., T.S., O.Y., D.R.S., R.K.J., and L.X. designed research; Y. Zhao, J.C., A.M., M.W., A.G., D.J., H.T.N., Y. Zhang, T.S., A.S.K., F.M., M.D., Y.S., L.W., X.G., O.Y., M.G.d.C., and L.X. performed research; Y. Zhao, J.C., A.M., M.W., A.G., D.J., H.T.N., Y. Zhang, T.S., A.S.K., F.M., M.D., Y.S., L.W., X.G., O.Y., M.G.d.C., D.R.S., R.K.J., and L.X. analyzed data; and Y. Zhao, J.C., A.M., M.W., D.J., H.T.N., T.S., M.D., O.Y., D.R.S., R.K.J., and L.X. wrote the paper.

Reviewers: J.H., The Ohio State University Wexner Medical Center; and F.Y., Duke University.

Conflict of interest statement: R.K.J. received an honorarium from Amgen; consultant fees from Merck, Ophthotech, Pfizer, SPARC, SynDevRx, and XTuit; owns equity in Enlight, Ophthotech, and SynDevRx; and serves on the boards of trustees of Tekla Healthcare Investors, Tekla Life Sciences Investors, Tekla Healthcare Opportunities Fund, and Tekla World Healthcare Fund. Neither any reagent nor any funding from these organizations was used in this study.

[1]Present address: Cancer Center, Union Hospital, Tongji Medical College, Huazhong University of Science and Technology, Wuhan, 430023 Hubei, China.

[2]Present address: Department of Obstetrics and Gynecology, Beijing TongRen Hospital, Capital Medical University, 100730 Beijing, China.

[3]Present address: Department of Oral and Maxillofacial Surgery, Xiangya Hospital, Central South University, Changsha, 410008 Hunan, China.

[4]To whom correspondence may be addressed. Email: jain@steele.mgh.harvard.edu or lei@steele.mgh.harvard.edu.

This article contains supporting information online at www.pnas.org/lookup/suppl/doi:10.1073/pnas.1818357116/-/DCSupplemental.

Published online January 18, 2019.

The renin–angiotensin system (RAS) is known for its pivotal role in maintaining cardiovascular homeostasis as well as fluid and electrolyte balance (15). Angiotensin II (AngII) was initially discovered as a vasoconstrictor, but is also known to contribute to the formation of the ECM (15). In ovarian cancer patients, it has been shown that (*i*) the level of tumor fibrosis inversely correlates with recurrence-free survival and overall survival (16), (*ii*) the serum level of angiotensin-converting enzyme (ACE), which converts inactive angiotensin I to the bioactive AngII, is elevated (17), and (*iii*) AT1 expression is associated with poor patient outcome (18, 19). Losartan is a Food and Drug Administration (FDA)-approved antihypertensive agent that blocks angiotensin II receptor type 1 (AT1). In mouse models of breast cancer and pancreatic cancer, losartan decreased the intratumoral expression of thrombospondin-1 (THBS-1), an activator of the fibrogenic TGF-β, and significantly reduced the intratumoral collagen and hyaluronan content. As a consequence solid stress was reduced, vessel compression was alleviated, and vascular perfusion was enhanced, resulting in reduced tumor hypoxia and improved delivery and efficacy of both low-molecular-weight drugs and nanomedicine (9, 20). These studies led to a successful phase II trial of losartan combined with chemoradiation in locally advanced pancreatic cancer (21). Whether losartan can modify the ovarian cancer tumor microenvironment and enhance chemotherapy efficacy is not known.

Chemotherapeutic agents may be given i.v. or through the i.p. route in ovarian cancer. Here, we hypothesize that by decreasing fibrosis in ovarian cancer, losartan should improve the delivery of drugs via both routes. First, by reducing solid stress, the resulting blood vessel decompression should improve delivery of blood-borne drugs to tumors. Second, since dense ECM can also hinder the penetration of large molecules and nanoparticles, such as monoclonal antibodies and Doxil, in tumors from the peritoneal surface (22), losartan should also improve the penetration of large therapeutics from the peritoneal cavity into ovarian tumors.

We report here that losartan used as an adjunctive treatment in murine models of ovarian cancer improves chemotherapeutic efficacy and decreases the related malignant ascites. We also report potential molecular mechanisms that may be used to develop biomarkers to predict response or development of resistance to chemotherapy. Finally, our retrospective analysis shows that patients with ovarian cancer who underwent concomitant treatment with an ACE inhibitor (ACEi) or angiotensin receptor blocker (ARB) in addition to standard of care demonstrate significantly enhanced overall survival compared with patients on other forms of antihypertensives.

Results

Losartan Treatment Reduces ECM Content in Ovarian Tumors. We first confirmed that AT1, the target for losartan, is expressed in our ovarian cancer cell lines (*SI Appendix*, Fig. S1*A*). Next, we determined if AT1 blockade by losartan treatment led to changes in ECM content. Mice were implanted with two human ovarian cancer cells, SKOV3ip1 and Hey-A8, orthotopically into the peritoneal cavity. To monitor peritoneal tumor growth, both cell lines were transduced with secretive Gaussia luciferase reporter gene (G-luc). Between 7 and 10 d after implantation when the blood G-luc value reached 2×10^6 relative light units (RLU), mice were randomized into control and losartan (40 mg/kg, once daily) treatment groups. i.p. injection of cancer cells resulted in solid tumors growing on the surface of the peritoneal organs and invading into the diaphragm. Mice bearing SKOV3ip1 tumors also produced a large amount of ascites. Tumor tissues were collected on day 28 postimplantation and evaluated for ECM content. We found that losartan treatment significantly reduced collagen and hyaluronan levels in both SKOV3ip1 and Hey-A8 tumors as indicated by histological analysis and by cDNA array (Fig. 1 *A* and *B* and *SI Appendix*, Fig. S1*B*).

Fibroblasts are the primary source of ECM proteins in both normal and malignant tissues (23, 24). In both SKOV3ip1 and Hey-A8 models, we found that losartan treatment significantly decreased the number of intratumoral αSMA-positive stromal cells, the main cellular components among which are the fibrogenic fibroblasts (Fig. 1*C*). Losartan treatment significantly reduced the expression of matrix molecules, including collagen (Col)-I and III, alpha smooth muscle actin (Acta2), and integrin beta (Itgb)-3 and -6. However, it did not significantly reduce the expression of major fibrogenic genes, including CTGF, PDGF-β, TGF-β1, and Thbs-1 as analyzed by pathway-specific cDNA array (ECM and adhesion molecule array) (*SI Appendix*, Fig. S1*B*).

Losartan Treatment Lowers Solid Stress in Ovarian Cancer. Since reduction in matrix is known to decrease solid stress (9, 25), we next investigated the effects of losartan treatment on solid stress in peritoneal ovarian tumors using the planar-cut technique

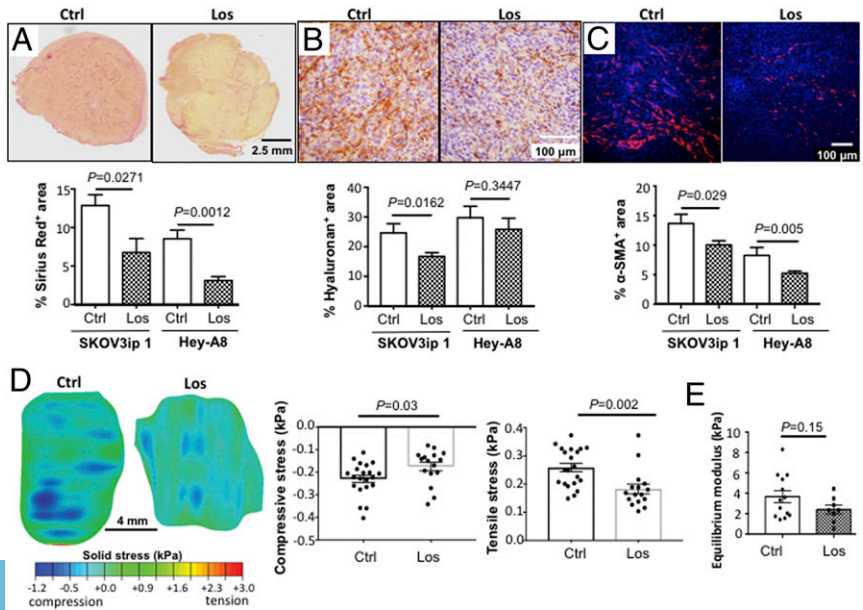

Fig. 1. Losartan treatment reduces matrix content, fibroblast infiltration, and solid stress in SKOV3ip1 and Hey-A8 ovarian cancer models. Control and losartan-treated human ovarian SKOV3ip1 and Hey-A8 tumors were stained for (*A*) collagen by Sirius Red staining, (*B*) hyaluronan by hyaluronic acid binding protein (HABP) staining, and (*C*) fibroblasts by αSMA staining. The fractions of Sirius Red (*A*, red), HABP (*B*, brown) and αSMA (*C*, red) positive areas were quantified using ImageJ software. All representative images shown are from SKOV3ip1 tumors. Data presented are mean ± SD. For each stain, $n = 12$ sections, with three sections per tumor. (*D*) Representative maps and quantification of compressive and tensile solid stresses in size-matched control and losartan-treated peritoneal SKOV3ip1 tumors. (*E*) The equilibrium modulus (stiffness) in control and losartan-treated peritoneal tumors.

(11, 25). In size-matched peritoneal SKOV3ip1 tumors, losartan treatment led to significant reduction in solid stress (Fig. 1*D*) and a trend toward decrease in matrix equilibrium modulus (stiffness) (Fig. 1*E*) and instantaneous modulus (*SI Appendix*, Fig. S2*B*). These results suggest that losartan treatment, via its antifibrotic effects, may be capable of decompressing vessels by reducing solid stress.

Losartan Treatment Improves Perfusion and Relieves Tumor Hypoxia. To determine whether the decrease in ECM content translated into decompressed vessels and improved vessel perfusion, we measured the fraction of perfused vessels and the level of tumor hypoxia by immunohistology. Losartan treatment did not change VEGF levels or microvessel density (*SI Appendix*, Fig. S1*C*) but significantly increased the percentage of perfused blood vessels (Fig. 2*A*). Following improved vessel perfusion, we found that the hypoxic fraction (evaluated via pimonidazole) of the viable ovarian carcinoma tissue was significantly reduced in losartan-treated tumors (Fig. 2*B*).

Losartan Treatment Increases Delivery of Chemotherapeutics. Decompression of blood vessels and improvements in vascular perfusion can enhance the delivery and intratumoral distribution of chemotherapeutic drugs in tumors (8–10). Pegylated liposomal doxorubicin is an FDA-approved treatment for patients with recurrent ovarian cancer which has demonstrated activity in both platinum-sensitive and platinum-resistant disease (26). Doxorubicin is autofluorescent; therefore, we used free doxorubicin as a tracer to study drug delivery in mouse models of ovarian cancer. In the control groups doxorubicin fluorescence signal was detected only proximal to blood vessels, whereas in losartan-treated mice fluorescence signal was broadly distributed throughout the tumor. Quantitative analysis confirmed that losartan treatment significantly increased the amount of intratumoral doxorubicin (red fluorescent signal) (Fig. 2*C*).

Mathematical Modeling Reproduces Losartan-Enhanced Drug Delivery and Predicts that Combined Losartan Treatment Will Improve Chemotherapy Efficacy. We have previously combined animal model studies with mathematical modeling to quantitatively predict drug delivery and to provide deeper insight into how the physiological barriers affect drug delivery (27). To further support the robustness of our observation that losartan increases the delivery of chemotherapeutics and enhances their efficacy, we developed a mathematical model (description in *SI Appendix*, *Materials and Methods* and Fig. S3). Informed by the experimental data of losartan-induced changes in the ECM content and doxorubicin delivery, our mathematical model reproduced the experimentally observed losartan effects on (*i*) the reduction of solid stress, (*ii*) the improvement of vascular perfusion, and (*iii*) the increase in intratumoral distribution of doxorubicin (Fig. 3 *A–D*).

In some cases of ovarian cancer, chemotherapy is directly administered i.p. (28). Using our mathematical model, we next investigated whether by reducing the matrix content losartan can directly affect the delivery and homogeneous distribution of a peritoneally administered drug into the peritoneal tumors. Peritoneally administered drugs can reach the tumor both by penetrating the tumor from the periphery and by being absorbed by blood vessels of the peritoneum and reach the tumor through the tumor vasculature. Physiological barriers that can hinder drug transport are (*i*) the dense tumor ECM that slows the direct diffusion (penetration) of macromolecules into the tumor from the peritoneal fluid, (*ii*) the solid stress that is accumulated during tumor growth and affects tumor blood vessel function by compressing vessels, and (*iii*) the hydraulic conductivity of the tumor, which is a measure of the tissue resistance to interstitial fluid flow and affects interstitial fluid pressure (22). A low hydraulic conductivity increases the tumor interstitial fluid pressure, and thus macromolecules have to penetrate from the peritoneal cavity into the tumor against a pressure gradient. Our model predicted that losartan treatment (*i*) reduced interstitial fluid pressure, (*ii*) increased the intratumoral delivery of oxygen, (*iii*) improved the intratumoral distribution of the i.p. administered first-line ovarian cancer chemotherapy drug paclitaxel, and (*iv*) resulted in a lower tumor volume when combined with chemotherapy (Fig. 3 *E–H*). We further performed a parametric analysis, varying drug's diffusivity, the elastic modulus of the tumor (which in the model regulates solid stress levels), and the tumor hydraulic conductivity to get insights about their relative contribution to peritoneal drug delivery. We found that an increase in the diffusivity of the drug or a decrease in tumor elastic modulus/solid stress levels can enhance considerably

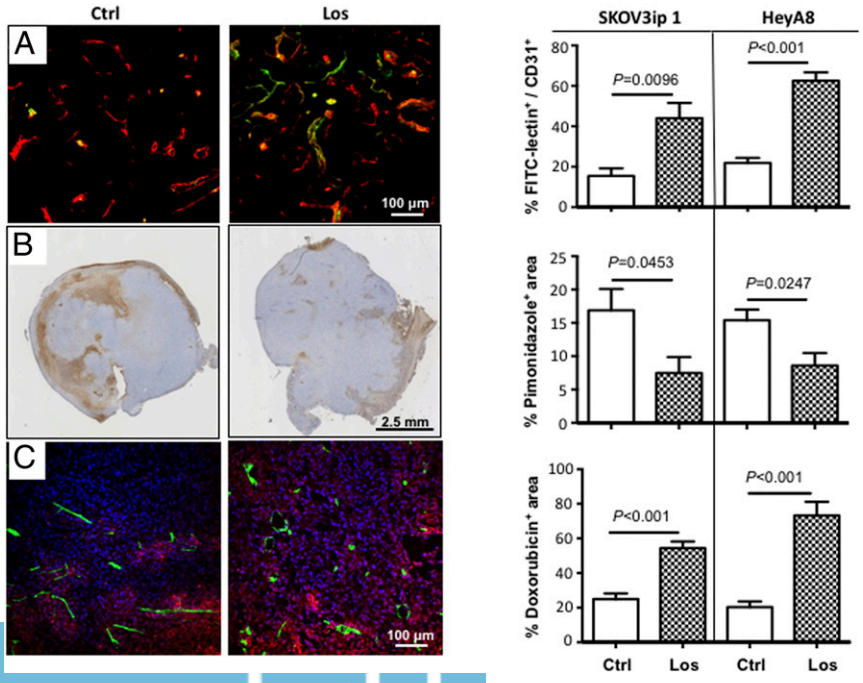

Fig. 2. Losartan treatment improves vessel perfusion, relieves tumor hypoxia, and increases drug delivery. Control and losartan-treated human ovarian SKOV3ip1 and Hey-A8 tumors were stained for (*A*) perfused (FITC-lectin$^+$, green) and total blood vessels (CD31$^+$ endothelial cells, red) and (*B*) hypoxic tumor tissues by pimonidazole stain (brown). The fraction of FITC-lectin$^+$/CD31$^+$ and hypoxic area was quantified using ImageJ software. (*C*) Representative images of doxorubicin intratumoral distribution and quantification of the fraction of tumor area positive for doxorubicin. Green, FITC-lectin labeled perfused vessels; red, fluorescent doxorubicin; blue, DAPI. All representative images shown are from SKOV3ip1 model. Data presented are mean ± SD. For each stain, n = 12 sections, with three sections per tumor.

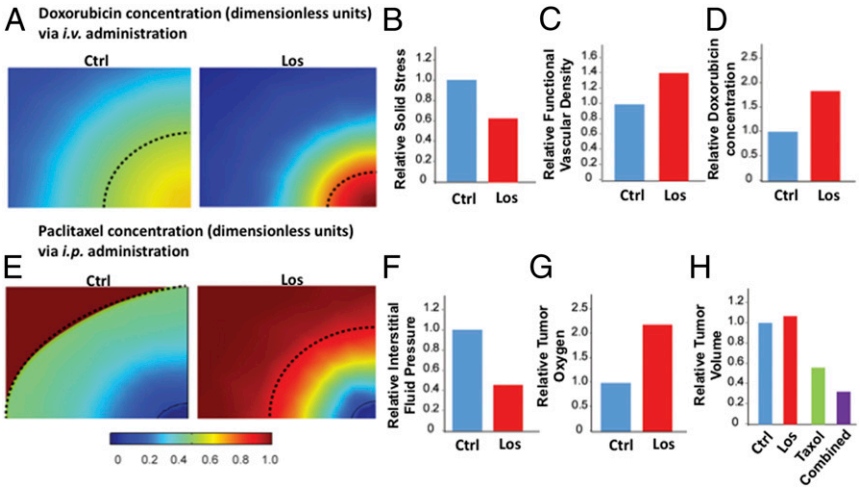

Fig. 3. Mathematical model based on losartan's mechanism of improved therapy. Model results for (*A*) the spatial intratumoral distribution of the cytotoxic drug doxorubicin following i.v. injection with and without losartan treatment. A 2D slice of the 3D model is presented; the dashed line denotes the interface of the tumor with the peritoneum. Model results for the relative change in the average (*B*) solid stress levels, (*C*) functional vascular density, (*D*) doxorubicin delivery, (*E*) delivery of i.p. administered paclitaxel, (*F*) fluid pressure at the tumor center, and (*G*) average tumor oxygen concentration with and without losartan treatment. (*H*) Predictions of the relative change in tumor volume for the treatment groups employed in the experimental study.

intratumoral drug distribution compared with the hydraulic conductivity (Fig. 4). The model also predicted that losartan can improve the delivery of both the i.v. administered paclitaxel as well as the i.p. administered doxorubicin (*SI Appendix*, Fig. S4).

Losartan Treatment Enhances Chemotherapeutic Efficacy in Ovarian Cancer Models. Based on the mathematical modeling predictions, we next determined whether losartan-induced changes in the ECM and blood vessels would enhance efficacy of i.p. paclitaxel, which is part of the first-line therapy for ovarian cancer, used by both the i.v. and i.p. routes. In both SKOV3ip1 and Hey-A8 models, mice were randomized into four treatment groups receiving (*i*) control, (*ii*) losartan, (*iii*) paclitaxel, or (*iv*) losartan combined with paclitaxel. In paclitaxel-treated mice, we found that peritoneal tumors were ~50% smaller compared with those in the control group. Losartan treatment alone did not affect the tumor growth; however, when it was combined with paclitaxel, it significantly enhanced the antitumor effect of i.p. paclitaxel in both SKOV3ip1 (Fig. 5*A*) and Hey-A8 (Fig. 5*D*) models. In the SKOV3ip1 model, which develops a significant amount of bloody ascites, losartan treatment significantly reduced the incidence and the amount of ascites (Fig. 5 *B* and *C*). In paclitaxel-treated tumors, we found that the number of proliferating tumor cells ($PCNA^+$) decreased and the number of apoptotic tumor cells ($TUNEL^+$) increased compared with the control group. In the combined treatment group, these changes were even more pronounced compared with the paclitaxel-alone group (Fig. 5 *E* and *F* and *SI Appendix*, Fig. S1 *D* and *E*).

Losartan Treatment Decreased Collagen Content and "Normalized" Lymphatic Vessel Networks in the Diaphragm. Tumors invading the diaphragm collapse local lymphatic vessels, leading to impaired abdominal fluid drainage and accumulation of ascites fluid (29).

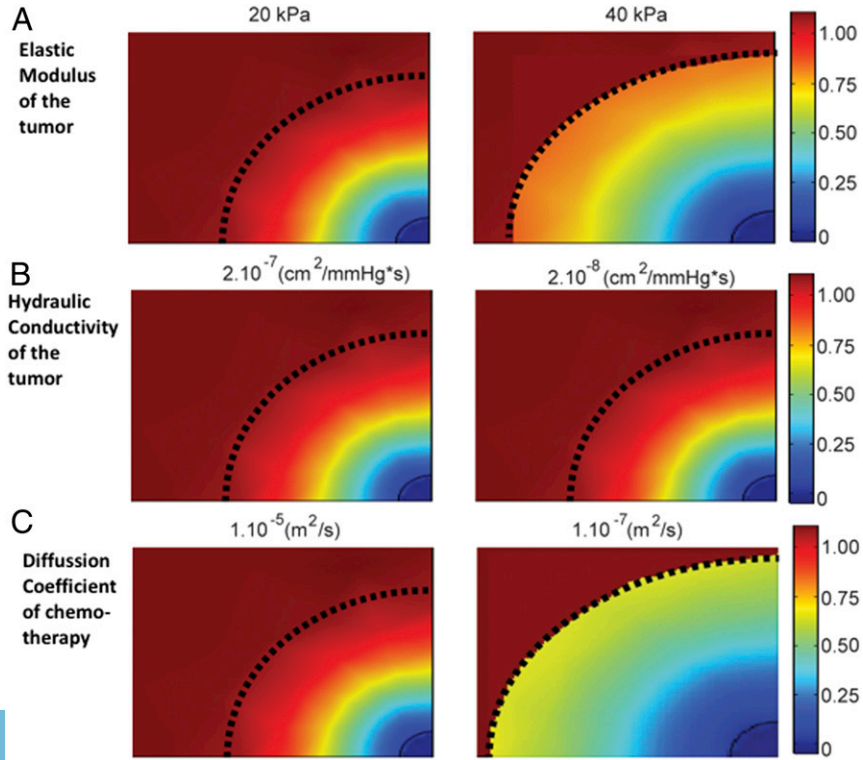

Fig. 4. Parametric analysis for the spatial intratumoral distribution of the drug following i.p. administration. The elastic modulus (*A*), hydraulic conductivity of the tumor (*B*), and the diffusion coefficient of the drug (*C*)—parameters that are known to affect drug delivery—were varied and model predictions from a slice of the 3D tumor model are presented.

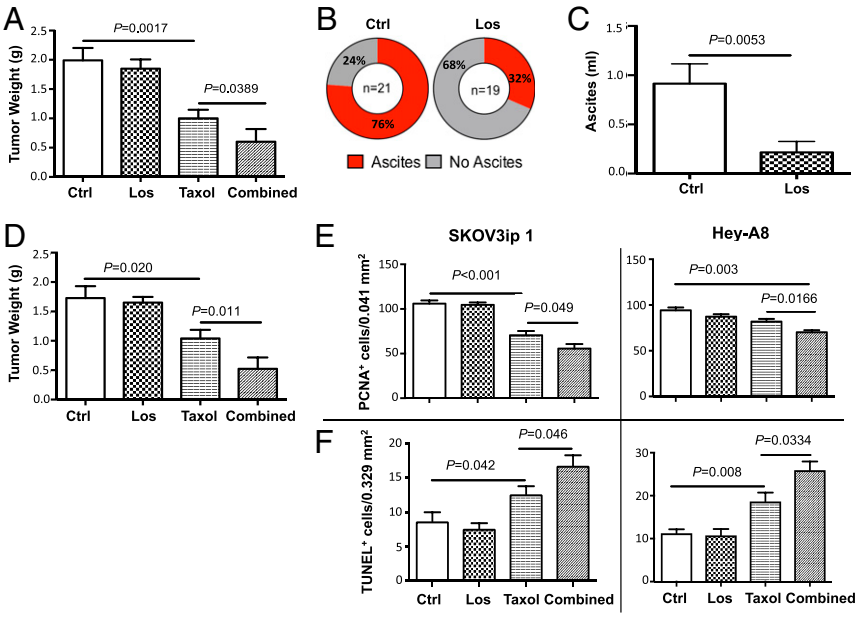

Fig. 5. Combined losartan treatment enhances the efficacy of paclitaxel. Mice were injected i.p. with SKOV3ip1 (*A*–*C*) and Hey-A8 (*D*) tumors, and peritoneal tumor growth was monitored by G-luc value. Between 7 and 10 d after implantation when peripheral blood G-luc value reached 2×10^6 RLU, mice were randomized into four treatment groups receiving (*i*) control (saline), (*ii*) losartan, (*iii*) paclitaxel, or (*iv*) losartan combined with paclitaxel. When mice became moribund, all peritoneal tumors were collected and weighed. The incidence (*B*) and volume (*C*) of ascites in SKOV3ip1 model were measured. Representative of at least three independent experiments (n = 10 each), data presented are mean ± SEM. (*E*) $PCNA^+$ tumor cells (per 0.041 mm^2), and (*F*) $TUNEL^+$ tumor cells (per 0.329 mm^2) were manually counted in 10 random fields in frozen sections of SKOV3ip1 and Hey-A8 tumors.

Although losartan monotherapy did not reduce tumor burden, it significantly decreased collagen content in size-matched diaphragm tumors (Fig. 6 *A* and *B*), suggesting a decreased solid stress. To assess effects on the diaphragm lymphatic vessels, we injected a fluorescent tracer (FITC-dextran) i.p. and directly visualized diaphragm lymphatic vessels by lymphangiography (29). In non-tumor-bearing mice, the normal lymphatic vessels displayed a network with organized branching on both the pleural and peritoneal sides of the diaphragm (Fig. 6*C*). In mice bearing SKOV3ip1 tumors (*i*) on the pleural side of the diaphragm, an enlarged network of lymphatic vessels was seen, indicating lymphatic network responding to increased fluid burden in the abdomen and potentially blockade of lymph flow, and (*ii*) on the peritoneal side the classical structure of lymphatic strips was completely disrupted. Strikingly, in mice treated with losartan, on both pleural and peritoneal sides of the diaphragm we found that the lymphatic vessel morphology was closer to that in normal non-tumor-bearing mice. The effects of losartan treatment on decreasing lymphatic vessel diameter on the pleural side were confirmed by image quantification (Fig. 6*D*). These lymphatic vessel morphological changes were further confirmed using double immunofluorescent staining for LYVE-1 and CD31 in whole-mount diaphragms (Fig. 6*E*).

Losartan Treatment Improves Lymphatic Vessel Function. Next, we used two tests to study the lymphatic drainage function. First, we injected fluorescent beads (1 μm in diameter) i.p. Two hours postinjection (*i*) in non-tumor-bearing mice very few fluorescent beads were found in the diaphragm, indicating clearance by functional lymphatics, (*ii*) in mice with SKOV3ip1 tumors a significant amount of fluorescent beads were retained in the diaphragm, suggesting impaired lymphatic drainage, and (*iii*) in losartan-treated mice some beads were retained within the lymphatic vessels, but significantly less than in control tumors, indicating improved lymphatic drainage (Fig. 7*A*).

Second, as diaphragm lymphatic vessels drain into the caudal mediastinal lymph nodes (CMLN), we collected the CMLNs and evaluated the amount of fluorescent beads drained to CMLN. Compared with non-tumor-bearing mice with normal drainage, CMLNs from SKOV3ip1 tumor-bearing mice accumulated fewer fluorescent beads and showed lower fluorescence intensity, indicating decreased drainage. CMLNs from losartan-treated mice showed higher fluorescence intensity, closer to the level in normal non-tumor-bearing mice (Fig. 7 *B* and *C*), indicating losartan treatment improved drainage to lymph node.

Losartan Treatment Induces the Expression of Antifibrotic miRNAs. Because miRNAs have emerged as major regulators of fibrosis in several fibrotic diseases (30), we used an miRNA array to evaluate how losartan altered the miRNA expression profile in ovarian cancer models. We found that losartan treatment significantly up-regulated the expression of miR-1-3p, miR-133a-3p (miR-133), miR-29b, and miR-26b-5p and down-regulated the expression of seven other miRNAs (Fig. 8*A*). As miRNAs function by binding to the target sites in the 3′UTR in target genes to repress their expression, we studied the miRNAs that were up-regulated by losartan treatment, to investigate if they contribute to the losartan-mediated reduction of matrix molecules in ovarian cancer models.

We screened the potential targets of these miRNAs using computational target-predicting software (www.microrna.org/microrna/home.do and www.targetscan.org/vert_72/). We found that miR-133 potentially targets collagen IA1 (COL1A1), collagen VA3 (COL5A3), and collagen VIA3 (COL6A3) genes, and its binding sequence is conserved across species (Fig. 8*B*), suggesting functional importance of the binding site. miR-1 is clustered on the same chromosomal locus as miR-133 (18q11.2); although it is up-regulated by losartan, it has no binding sites on any of the matrix genes. miR-29 is a master regulator of fibrosis that has been shown to target at least 20 different ECM-related genes, including collagens, laminins, and integrins in RAS-mediated hypertensive cardiovascular diseases and renal disease (31–33). miR-29 is down-regulated in fibrotic conditions in multiple organs, including the heart, liver, kidney, and skin (32–34), and the fibrogenic TGF-β/Smad3 axis has been shown to suppress miR-29 expression (33, 35). miR-26 has no binding sites on any of the matrix genes. Thus, as miR-133 is most significantly induced by losartan treatment (>500-fold) in ovarian cancer model, we focused our study on miR-133.

Losartan Treatment Up-Regulates miR-133 Expression, Which Reduces Collagen I Levels in Human Ovarian Cancer Cells. Among the target genes of miR-133, the collagen I expression was significantly reduced by losartan treatment (*SI Appendix*, Fig. S1*B*). The *Col I* gene encodes the two pro-a1(I) chains in type I collagen, which is the most abundant form of matrix molecule present in the tumor

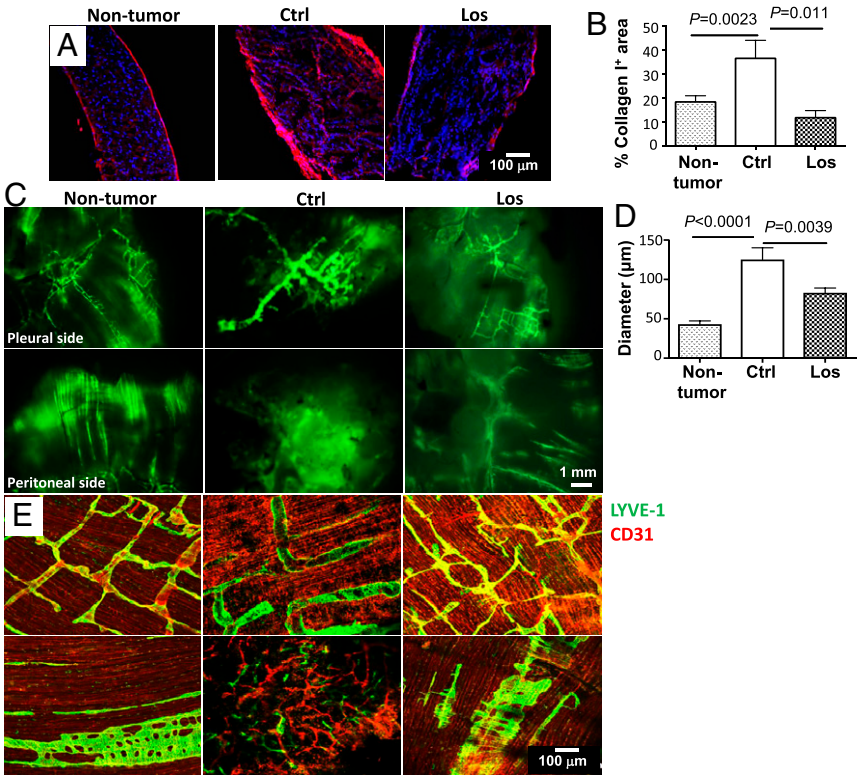

Fig. 6. Losartan reduces collagen content in the tumors invading the diaphragm and "normalizes" diaphragm lymphatic vessel morphology. Diaphragms from non-tumor-bearing mice and from mice bearing SKOV3ip1 tumors treated with control or losartan were collected. (*A*) Representative immunofluorescent staining images of collagen I (red) in cross-sectioned diaphragm. (*B*) The fraction of collagen I-positive area in the diaphragm was quantified using ImageJ software. (*C*) Representative images of fluorescent lymphangiography. In non-tumor-bearing mice, and mice bearing SKOV3ip1 tumors treated with control or losartan, FITC-dextran (green) were injected into the peritoneum to label lymphatic vessels on the pleural and peritoneal side of diaphragm. (*D*) Lymphatic vessel diameter on the pleural side of the diaphragm was quantified using ImageJ. (*E*) Representative immunofluorescent staining images of lymphatic vessels (LYVE-1-green and CD31-red) in whole-mounted diaphragm. Data presented are mean ± SD. For each staining, $n = 12$ sections, with three sections per tumor.

ECM. First, we confirmed that losartan increased the miR-133 level in SKOV3ip1 and Hey-A8 ovarian cancer cells, as well as in mouse fibroblast (10T1/2) and macrophage (Raw264.7) cell lines in vitro by TaqMan assay (*SI Appendix*, Fig. S5*A*). Next, to study if miR-133 reduces collagen level, we cloned pri-miR-133 by amplifying a 500-bp fragment spanning miR-133 stem–loop sequence from human genomic DNA. SKOV3ip1 cells were transduced to overexpress pri-miR-133 (529-fold compared with nontransfected cells). While overexpression of miR-133 did not change *Col1A1* mRNA levels (0.9 ± 0.2-fold compared with control), it significantly decreased collagen I protein levels (Fig. 8*C*).

To confirm that miR-133 directly binds to the predicted target site in the collagen I gene and led to its down-regulation, we cloned the predicted miR-133 target site from the *ColIA1* gene and inserted it into the 3′UTR of the firefly luciferase gene (pmiRGLO-ColI-wt; Fig. 8*D*). When miR-133 directly binds to the target sequence, it leads to mRNA destabilization or translational repression, resulting in reduced expression of firefly luciferase protein and low

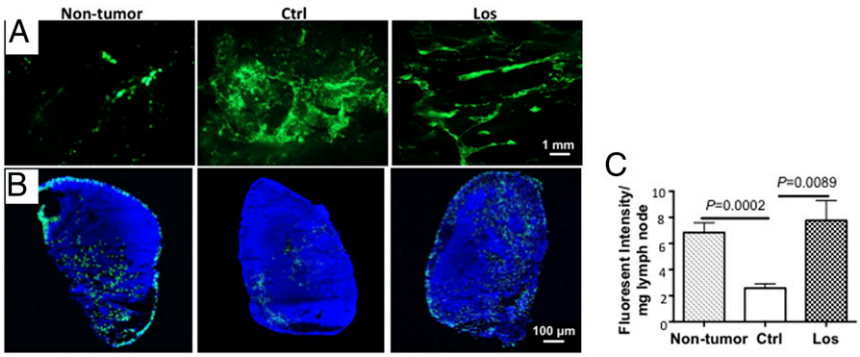

Fig. 7. Losartan improves diaphragm lymphatic vessel drainage. In non-tumor-bearing mice, and mice bearing SKOV3ip1 tumors treated with control or losartan, fluorescent beads (green) were injected into the peritoneum to observe their drainage. Representative images of (*A*) the diaphragm and (*B*) the CMLN frozen sections under confocal microscope. Blue, DAPI. (*C*) The amount of fluorescent beads drained to the CMLN was quantified by measuring the fluorescence intensity of homogenized CMLNs using a plate reader. Data presented are mean ± SD, $n = 12$ diaphragms and CMLNs each.

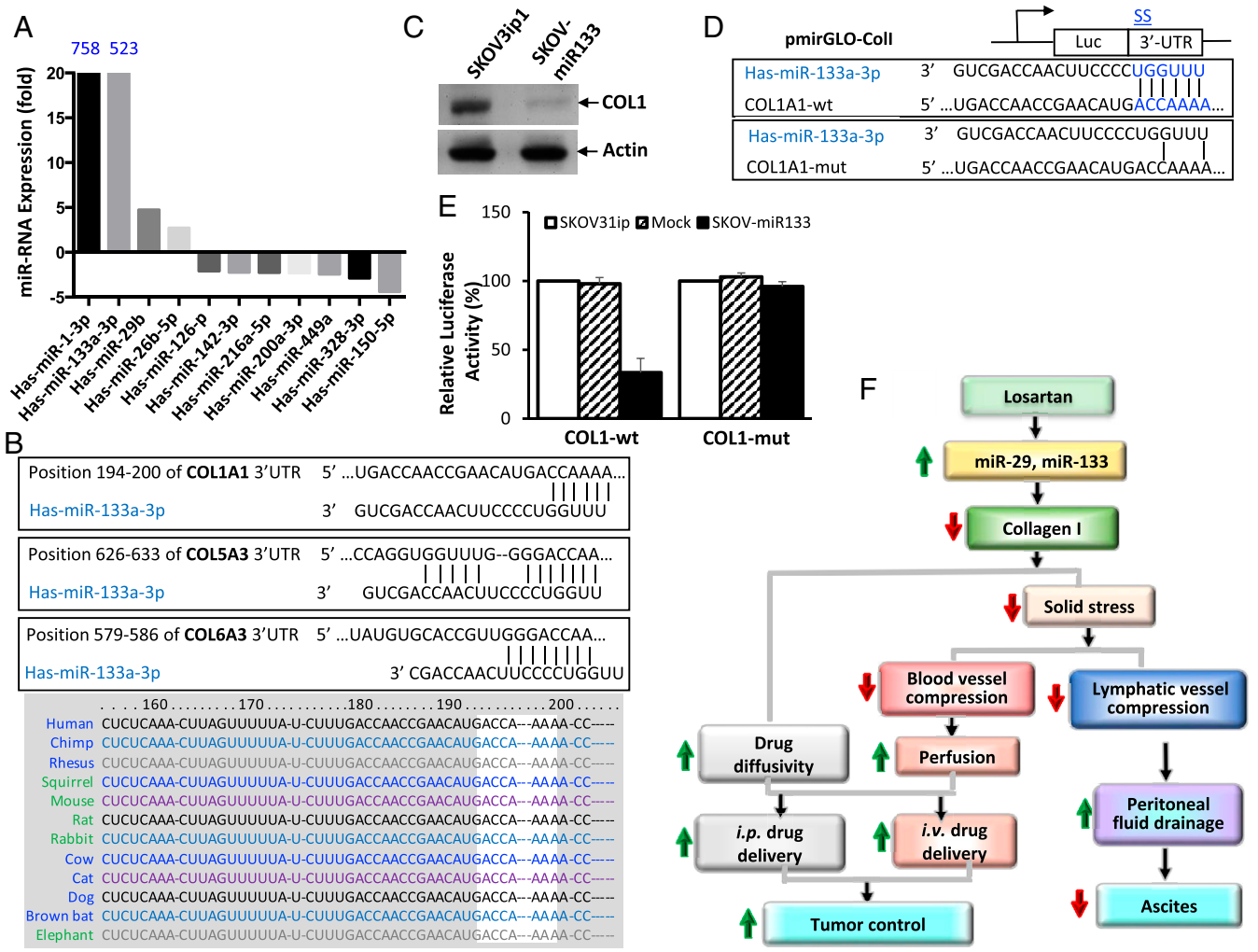

Fig. 8. Losartan treatment increases miR-133 level, which regulates collagen levels. (*A*) miRNAs differentially regulated in control and losartan-treated SKOV3ip1 cells as evaluated by miRNA array. (*B*, *Top*) Sequence alignment of miR-133 with the 3′UTR of the COL1A1, COL5A3, and COL6A3 genes. The noncoding RNA sequence of each gene and the seed sequence of hsa-miR-133-3p are shown. (*B*, *Bottom*) The seed sequence of miR-133 in COL1A1 is highly conserved among different species, including humans (*Homo sapiens*), mice (*Mus musculus*), and rats (*Rattus norvegcus*). (*C*) Western blot of collagen I in parental and miR-133–overexpressing SKOV3ip1 cells. (*D*) Schematic representations of the luciferase reporter construct with the locations of the seed sequence (SS) in the COL1A1 3′-UTR. Potential base pairs between hsa-miR-133 and the target site are indicated in the wild-type and mutated seed sequence. (*E*) Relative luciferase activity. Parental, mock, and miR-133–overexpressing SKOV3ip1 cells were transiently cotransfected with wild-type (pmirGLO-COL1-wt) or mutant (pmirGLO-COL1-mut) firefly luciferase reporter genes and Renilla luciferase genes. Firefly luciferase activities were normalized to Renilla luciferase activity. Data presented are mean ± SD. (*F*) Potential mechanisms by which losartan treatment enhanced chemotherapy efficacy and reduced ascites. Losartan treatment significantly up-regulates miRNAs that target collagen molecules, leading to reduced matrix content. Reduced matrix content can alleviate compression on vessels. As a result (*i*) blood vessel perfusion is significantly improved, leading to increased delivery of oxygen and drug and enhanced chemotherapy efficacy of blood-borne drugs and (*ii*) diaphragm lymphatic vessels drainage function is enhanced, leading to improved peritoneal fluid drainage and decreased accumulation of ascites.

chemiluminescent signal. To confirm whether the reduction of luciferase activity is a direct consequence of miR-133 binding to the target sequence in the *ColIA1* gene, we created a mutated target site, which causes decreased complementarity to miR-133 (pmiRGLO-ColI-mut; Fig. 8*D*). Parental, mock, and miR-133–overexpressing SKOV3ip1 cells were transiently transfected with these wild-type and mutated luciferase reporters and the Renilla luciferase reporter gene (as transfection efficiency control). In parental and mock-transfected SKOV3ip1 cells, the low level of endogenous miR-133 did not affect the luciferase activity. In cells that overexpress miR-133 (SKOV-miR133), large amounts of miR-133 presumably bind to the cloned wild-type *ColIA1* target site, leading to significant reduction of the luciferase activity. Mutation of the target site abolished the miR-133–mediated repression of luciferase activity (Fig. 8*E*), confirming that miR-133 directly targets *ColIA1* gene.

Finally, to study the biological role of miR-133 in vivo, we implanted (*i*) parental, (*ii*) mock, and (*iii*) pri-miR-133–overexpressing SKOV3ip1 cells into the peritoneal cavity of nude mice. miR-133 overexpression did not affect tumor growth but slightly decreased ascites (but did not reach statistical significance; *SI Appendix*, Fig. S5*B*). Histological analysis of the tumors revealed that miR-133 overexpression did not significantly change the collagen I content (15.4 ± 4.6% in SKOV3ip1 vs. 12.6 ± 2.8% in SKOV-miR133 tumors) (*SI Appendix*, Fig. S5*C*) or intratumoral doxorubicin distribution (24.4 ± 3.7% in SKOV3ip1 vs. 20.6 ± 4.4% in SKOV-miR133 tumors) (*SI Appendix*, Fig. S5*D*).

Use of an ACEi or ARB Is Associated with Increased Survival in Patients with Ovarian Cancer. We next sought to test the hypothesis that angiotensin pathway modulation would improve survival in patients with advanced-stage ovarian cancer concomitantly

receiving standard of care. We performed a retrospective analysis of patients with stage IIIC or IV ovarian cancer treated at Massachusetts General Hospital (MGH) and Brigham and Women's Hospital (BWH) between January 1, 2010 and December 31, 2014. We used inverse probability of treatment weighting based on propensity score to create a weighted cohort of patients who differed with respect to blood pressure medication use (ACEi/ARB versus betablocker/calcium channel blocker/diuretic) but were similar with respect to prognostic factors (*SI Appendix*, Table S1) such as age ($P = 0.88$), comorbidity index ($P = 0.95$), histology ($P = 0.92$), treatment approach ($P = 0.97$), and residual disease status ($P = 1$). In the weighted cohort, compared with patients using betablockers, calcium channel blockers, or diuretics, use of ACEi/ARB was associated with a significant reduction in hazard of death (hazard ratio 0.55, 95% CI interval 0.36–0.95; $P = 0.004$). Women taking an ACEi/ARB had a median survival of 63 mo compared with 33 mo among women taking another type of blood pressure medication (Fig. 9*A*). The robustness of the main analysis was assessed in several sensitivity analyses. To ensure that the main effect was not due to the survival effects from other antihypertensive medications, the main analysis was repeated after excluding patients using each of the following categories of antihypertensive: betablockers, calcium channel blockers, or diuretics (*SI Appendix*, Table S1). Furthermore, we assessed whether the effect of angiotensin blockade was evident among patients taking ACEi or ARB medications (*SI Appendix*, Table S2). Finally, we evaluated whether survival differed between patients using ACE or ARB medications. As shown in Fig. 9*B*, treatment with ARB was superior to ACEi treatment, consistent with data from our preclinical mouse models with losartan (9).

Discussion

Treatment difficulties in ovarian cancer include advanced-stage disease at diagnosis and the eventual development of chemoresistance (2–4). For patients with ovarian cancer who have a complete or partial response to platinum-based chemotherapy, there are now three poly ADP ribose polymerase (PARP) inhibitors (olaparib, niraparib, and rucaparib) approved for use in the maintenance setting (36, 37). However, for platinum-resistant patients, PARP inhibitors are less effective and combining PARP inhibitors with chemotherapy is challenging due to toxicity (38, 39). In recurrent ovarian cancer patients, bevacizumab, an anti-VEGF monoclonal antibody, is now FDA-approved (40–42). However, modest bevacizumab survival benefits, high cost, and the limited duration of response leave room for the development of better vascular targeting strategies.

The goals of our study were to investigate if losartan—an FDA-approved ARB—can normalize the tumor ECM, improve the delivery and efficacy of chemotherapies in ovarian cancer, and demonstrate any meaningful clinical benefits over cytotoxic therapy alone. We uncovered three major findings that can be clinically tested to potentially improve ovarian cancer treatment: (*i*) We developed a strategy targeting the tumor microenvironment by AT1 blockade to curb extrinsic chemoresistance and control ascites; (*ii*) we discovered that patients receiving either an ACEi or an ARB exhibited significantly longer overall survival compared with ovarian cancer patients on other antihypertensives; and (*iii*) we identified a fibrogenic miRNA signature that may serve as a biomarker of ovarian cancer chemotherapy resistance. We also developed a tool that may advance the research of drug delivery and development in ovarian cancer: Using a planar-cut method, we provided evidence that AT1 blockade reduces solid stress exerted from the dense tumor ECM, which in turn improves drug delivery.

Angiotensin II type 1 receptor blockers (ARBs), including losartan, candesartan, telmisartan, and valsartan, are commonly used in the clinic for the treatment of hypertension. Among the ARBs, losartan features ideal tissue distribution and penetration (43). Therefore, we used losartan to block AngII signaling in models of ovarian cancer—a highly desmoplastic cancer. In our ovarian cancer model, we did not observe direct cell proliferative effects from recombinant AngII treatment or growth inhibitory effect from losartan treatment in vitro, nor did we observe antitumor effects from losartan treatment in vivo. Instead, we found that losartan treatment enhanced the efficacy of paclitaxel by facilitating drug delivery through two mechanisms. First, using our newly developed technique, we showed that losartan treatment lowered solid stress that compresses and collapses blood vessels, leading to improved vessel perfusion and increased drug delivery. Second, using mathematical modeling, we showed that by decreasing the ECM content losartan increases the diffusivity (i.e., intratumoral penetration) of the i.p. or i.v. injected macromolecular drugs (e.g., albumin-bound chemotherapeutics, antibodies, and nanoparticles) into the peritoneal tumors. These dual mechanisms of improved drug delivery support the clinical testing of losartan as an adjunct therapy to enhance the efficacy of therapeutics given i.v. or i.p. in ovarian cancer (Fig. 8*F*). To fully characterize the chemosensitization capacity of losartan, further studies of combining losartan with other therapeutics, such as doxorubicin and PARP inhibitors, should be tested in the ovarian cancer models.

The majority of patients with stage III or IV ovarian cancer develop malignant ascites and suffer from symptoms such as

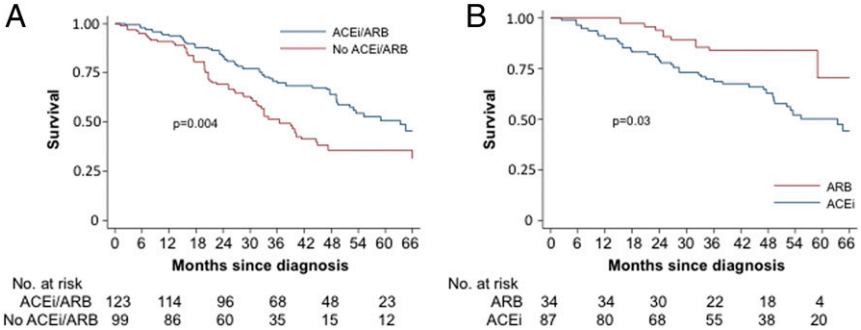

Fig. 9. ACEi/ARB adjunctive treatment improves survival in women with ovarian cancer receiving standard of care. (*A*) Inverse probability of treatment-weighted survival curves for patients with advanced ovarian cancer who were users of ACEis or ARBs (ACEi/ARB, blue line) compared with users of any other antihypertensive medication (No ACEi/ARB, red line) at the time of cytoreductive surgery. Hazard of death from any cause was significantly lower among women receiving an ACEi or ARB compared with controls (hazard ratio 0.55; 95% CI 0.36–0.95). (*B*) Inverse probability of treatment-weighted survival curves patients with advanced ovarian cancer who were users of ARBs (red line) compared with users of ACEis (blue line) at the time of cytoreductive surgery. Hazard of death from any cause was significantly lower among women receiving an ARB compared with ACEi (hazard ratio 0.38; 95% CI 0.15–0.91).

abdominal pressure and distension, dyspnea, bloating, pelvic pain, and bowel/bladder dysfunction (44, 45). A combination of increased production of peritoneal fluid from elevated expression of tumor VEGF (46) and decreased drainage through diaphragmatic lymphatic channels results in the accumulation of ascites. Platinum-based chemotherapy will usually reduce tumor burden and control malignant ascites during initial treatment. Unfortunately, in patients with chemotherapy-resistant advanced ovarian cancer, no consistently effective therapy has been identified, other than repetitive paracentesis. Losartan has been shown to decrease the expression of VEGF (15); however, in our study, we did not observe VEGF expression change after losartan treatment. While we did not investigate it, losartan may also decrease the expression of molecules other than VEGF that are responsible for ascites formation (15, 47). Previously, we reported that TGF-β blockade via reducing tumor burden in the diaphragm relieved the compression from the tumor mass on the diaphragm lymphatic vessels and improved their drainage of peritoneal fluid and resulted in reduced ascites in ovarian cancer models (29). The development of TGF-β pathway inhibitors has long been impeded by toxicity issues (48–50). However, several TGF-β inhibitors have now reached clinic trials with a safe toxicity profile (51, 52). In the current study, we showed a safer and less expensive strategy (less than $1 per d; ref. 53): Losartan reduced ascites by decreasing the ECM content in ovarian tumors invading the diaphragm, thus relieving solid stress and the compression on the diaphragm lymphatic vessels, improving drainage of the peritoneal fluid (Fig. 8*F*). Our results suggest that in patients with relapsed or refractory ovarian cancer where chemotherapy no longer has effect on tumor burden losartan may be an option for controlling ascites, relieving symptoms and improving life quality.

To evaluate the translational potential of angiotensin signaling blockade in patients with ovarian cancer, we queried our database consisting of 522 women who received surgery and chemotherapy at MGH and BWH. We compared 123 women receiving an ACEi/ARB to 99 women treated with other antihypertensive agents to minimize confounders related to underlying hypertension and frequency of medical visits and supportive care related to their underlying hypertension. Stated differently, this comparison allowed us to test the hypothesis that modulation of the angiotensin signaling specifically and not the general medical management of hypertension improves outcome in ovarian cancer. After controlling for independent factors that improve survival in this disease such as stage, histology, and residual disease, we found that treatment with an ACEi or ARB was associated with a 30-mo median survival benefit. Furthermore, treatment with an ARB was superior to ACEi, consistent with our proposed mechanisms (9). Despite the robustness of our analysis, we are limited by the retrospective nature of our analysis and the potential for other unmeasured confounders such as other concomitant medications and overall health status. However, the magnitude of effect of this readily accessible and relatively well-tolerated therapy deserves further investigation.

Recent evidence has suggested that miRNAs play a role in fibrotic disease (30). We found that, unlike in breast and pancreatic cancers (9, 20, 54), losartan treatment did not significantly change the expression of fibrogenic genes in ovarian tumors but significantly up-regulated miRNAs that target collagen family genes, including miR-29 and miR-133/miR-1 cluster. miR-29b is known to be a major regulator of fibrosis in multiple fibrotic models (55). The role of miR-133 on fibrosis is less well studied. In a hypertension model, miR-133 has been shown to reduce collagen I expression (56), in a diabetes model miR-133 overexpression has been shown to prevent cardiac fibrosis (57), and in a liver fibrosis model fibrogenic TGF-β has been shown to down-regulate miR-133 (58). In our study, losartan treatment increased miR-133 level in cancer cells, fibroblasts, and macrophages. We confirmed that miR-133 directly targets collagen I gene and leads to reduced collagen production in ovarian cancer cells. However, overexpression of miR-133 in cancer cells did not significantly change collagen levels in xenograft ovarian tumors. This may be due to the following reasons: (*i*) miR-133 only targeted collagen I, leaving the other fibrogenic signaling pathways intact and sustaining matrix production, and (*ii*) when miR-133 expression is only modified in ovarian cancer cells the production of matrix molecules by matrix-producing tumor-associated stromal cells (such as fibroblasts and macrophages) is not affected, and they maintain their matrix production. The use of angiotensin II type 1a receptor (AT1) knockout mice (59–61) would be a useful tool to fully profile the miRNAs mediating matrix production—comparison of miRNAs expressed in ovarian tumors grown in wild-type mice vs. those grown in AT1 knockout mice would generate an RAS-regulated matrix-targeting miRNA signature.

Another potential clinical application of our finding is that a panel of antifibrotic miRNAs could potentially be explored as candidate biomarkers of response to chemotherapy and the development of chemoresistance. However, these candidate biomarkers need to be validated prospectively in independent clinical trials. Ovarian cancer is a silent disease of usually late diagnosis, and patient response to treatment is difficult to predict. There is a serious need for biomarkers to orient treatment choices and reflect tumor response. Due to their small size and stability, circulating miRNAs can be reliably detected and quantified and have been shown to reflect the expression pattern observed in the tumor tissues, highlighting their potential use as easily detectable tumor biomarkers (62–64). While serum levels of miRNAs are accepted biomarkers for liver disease (65), whether the panel of antifibrotic miRNAs in ascites have the potential to be used as biomarkers is unknown. Our study indicates a strong rationale to develop an ascites miRNA screening diagnostic for biomarkers of response to chemotherapy and the development of chemoresistance.

In summary, our study demonstrates that integrating a matrix-depleting strategy with chemotherapy in ovarian cancer models enhances chemotherapy efficacy and reduces ascites. These findings can be rapidly tested in a prospective clinical trial.

Methods

The effects of losartan on tumor microenvironment, drug delivery, and chemotherapy efficacy were studied in two orthotopic ovarian cancer models. For additional information regarding drug delivery, treatment protocols, patient characteristics, and stastical analysis, see *SI Appendix, Materials and Methods*.

Retrospective analysis of patients with stage IIIC or IV ovarian cancer treated at MGH and BWH between January 1, 2010 and December 31, 2014 was performed in accordance with MGH Institutional Review Board approval. All animal procedures were performed following the guidelines of Public Health Service Policy on Humane Care of Laboratory Animals and approved by the Institutional Animal Care and Use Committee of MGH.

ACKNOWLEDGMENTS. We thank ShanMin Chin, Anna Khachatryan, and Carolyn Smith for their superb technical support; Dr. Peigen Huang for his help on animal studies; Dr. Nilesh Talele for help with the solid stress; and Drs. Yves Boucher and Timothy Padera for helpful discussions. This work was supported by Department of Defense New Investigator Award W81XWH-16-1-0219 (to L.X.); American Cancer Society Research Scholar Award RSG-12-199-01-TBG (to L.X.); Children's Tumor Foundation Drug Discovery Initiative (L.X.); an Ira Spiro Award (L.X.); Burroughs Wellcome Fund Postdoctoral Enrichment Award (D.J.); NIH Grants F32-CA216944-01 (to H.T.N.) and F31-HL126449 (to M.D.); an A*STAR Fellowship (A.S.K.); European Research Council Grant ERC-2013-StG-336839 (to T.S.); NIH Grant P01-CA190174 (to D.R.S. and O.Y.); NIH Grants P01-CA080124, P50-CA165962, R01-CA129371, R01-CA208205, and U01-CA224348; and National Cancer Institute Outstanding Investigator Award R35-CA197743, the Jane's Trust Foundation, the Lustgarten Foundation, the Ludwig Center at Harvard, the National Foundation for Cancer Research, and the Gates Foundation (to R.K.J.).

1. Siegel RL, Miller KD, Jemal A (2018) Cancer statistics, 2018. *CA Cancer J Clin* 68:7–30.
2. Christie EL, Bowtell DDL (2017) Acquired chemotherapy resistance in ovarian cancer. *Ann Oncol* 28(Suppl_8):viii13–viii15.
3. Coleman RL, Monk BJ, Sood AK, Herzog TJ (2013) Latest research and treatment of advanced-stage epithelial ovarian cancer. *Nat Rev Clin Oncol* 10:211–224.
4. Karam A, et al.; Participants of the 5th Ovarian Cancer Consensus Conference (2017) Fifth ovarian cancer consensus conference of the gynecologic cancer interGroup: First-line interventions. *Ann Oncol* 28:711–717.
5. Jain RK (1997) Delivery of molecular and cellular medicine to solid tumors. *Adv Drug Deliv Rev* 26:71–90.
6. Yuan F (1998) Transvascular drug delivery in solid tumors. *Semin Radiat Oncol* 8:164–175.
7. Stylianopoulos T, et al. (2012) Causes, consequences, and remedies for growth-induced solid stress in murine and human tumors. *Proc Natl Acad Sci USA* 109:15101–15108.
8. Liu J, et al. (2012) TGF-β blockade improves the distribution and efficacy of therapeutics in breast carcinoma by normalizing the tumor stroma. *Proc Natl Acad Sci USA* 109:16618–16623.
9. Chauhan VP, et al. (2013) Angiotensin inhibition enhances drug delivery and potentiates chemotherapy by decompressing tumour blood vessels. *Nat Commun* 4:2516–2527.
10. Jain RK (2013) Normalizing tumor microenvironment to treat cancer: Bench to bedside to biomarkers. *J Clin Oncol* 31:2205–2218.
11. Nia HT, et al. (2016) Solid stress and elastic energy as measures of tumour mechanopathology. *Nat Biomed Eng* 1:4–29.
12. Jain RK, Martin JD, Stylianopoulos T (2014) The role of mechanical forces in tumor growth and therapy. *Annu Rev Biomed Eng* 16:321–346.
13. Stylianopoulos T, Munn LL, Jain RK (2018) Reengineering the physical microenvironment of tumors to improve drug delivery and efficacy: From mathematical modeling to bench to bedside. *Trends Cancer* 4:292–319.
14. Jain RK (2014) Antiangiogenesis strategies revisited: From starving tumors to alleviating hypoxia. *Cancer Cell* 26:605–622.
15. Pinter M, Jain RK (2017) Targeting the renin-angiotensin system to improve cancer treatment: Implications for immunotherapy. *Sci Transl Med* 9:eaan5616.
16. Samrao D, et al. (2012) Histologic parameters predictive of disease outcome in women with advanced stage ovarian carcinoma treated with neoadjuvant chemotherapy. *Transl Oncol* 5:469–474.
17. Beyazit F, Ayhan S, Celik HT, Gungor T (2015) Assessment of serum angiotensin-converting enzyme in patients with epithelial ovarian cancer. *Arch Gynecol Obstet* 292:415–420.
18. Ino K, et al. (2006) Angiotensin II type 1 receptor expression in ovarian cancer and its correlation with tumour angiogenesis and patient survival. *Br J Cancer* 94:552–560.
19. Song L, et al. (2013) Serum agonistic autoantibodies against type-1 angiotensin II receptor titer in patients with epithelial ovarian cancer: A potential role in tumor cell migration and angiogenesis. *J Ovarian Res* 6:22–28.
20. Diop-Frimpong B, Chauhan VP, Krane S, Boucher Y, Jain RK (2011) Losartan inhibits collagen I synthesis and improves the distribution and efficacy of nanotherapeutics in tumors. *Proc Natl Acad Sci USA* 108:2909–2914.
21. Murphy JE, et al. (2018) Potentially curative combination of TGF-b1 inhibitor losartan and FOLFIRINOX (FFX) for locally advanced pancreatic cancer (LAPC): R0 resection rates and preliminary survival data from a prospective phase II study. *J Clin Oncol* 36(15_Suppl):4116–4116.
22. Netti PA, Berk DA, Swartz MA, Grodzinsky AJ, Jain RK (2000) Role of extracellular matrix assembly in interstitial transport in solid tumors. *Cancer Res* 60:2497–2503.
23. Öhlund D, Elyada E, Tuveson D (2014) Fibroblast heterogeneity in the cancer wound. *J Exp Med* 211:1503–1523.
24. Schwarz RI (2015) Collagen I and the fibroblast: High protein expression requires a new paradigm of post-transcriptional, feedback regulation. *Biochem Biophys Rep* 3:38–44.
25. Nia HT, et al. (2018) Quantifying solid stress and elastic energy from excised or in situ tumors. *Nat Protoc* 13:1091–1105.
26. Green AE, Rose PG (2006) Pegylated liposomal doxorubicin in ovarian cancer. *Int J Nanomedicine* 1:229–239.
27. Chauhan VP, et al. (2012) Normalization of tumour blood vessels improves the delivery of nanomedicines in a size-dependent manner. *Nat Nanotechnol* 7:383–388.
28. Armstrong DK, et al.; Gynecologic Oncology Group (2006) Intraperitoneal cisplatin and paclitaxel in ovarian cancer. *N Engl J Med* 354:34–43.
29. Liao S, et al. (2011) TGF-beta blockade controls ascites by preventing abnormalization of lymphatic vessels in orthotopic human ovarian carcinoma models. *Clin Cancer Res* 17:1415–1424.
30. O'Reilly S (2016) MicroRNAs in fibrosis: Opportunities and challenges. *Arthritis Res Ther* 18:11–20.
31. Pan J, et al. (2014) Role of microRNA-29b in angiotensin II-induced epithelial-mesenchymal transition in renal tubular epithelial cells. *Int J Mol Med* 34:1381–1387.
32. van Rooij E, et al. (2008) Dysregulation of microRNAs after myocardial infarction reveals a role of miR-29 in cardiac fibrosis. *Proc Natl Acad Sci USA* 105:13027–13032.
33. Qin W, et al. (2011) TGF-β/Smad3 signaling promotes renal fibrosis by inhibiting miR-29. *J Am Soc Nephrol* 22:1462–1474.
34. Maurer B, et al. (2010) MicroRNA-29, a key regulator of collagen expression in systemic sclerosis. *Arthritis Rheum* 62:1733–1743.
35. Wang B, et al. (2012) Suppression of microRNA-29 expression by TGF-β1 promotes collagen expression and renal fibrosis. *J Am Soc Nephrol* 23:252–265.
36. Mittica G, et al. (2018) PARP inhibitors in ovarian cancer. *Recent Pat Anticancer Drug Discov* 13:392–410.
37. Morgan RD, Clamp AR, Evans DGR, Edmondson RJ, Jayson GC (2018) PARP inhibitors in platinum-sensitive high-grade serous ovarian cancer. *Cancer Chemother Pharmacol* 81:647–658.
38. Lorusso D, et al. (2017) The safety of antiangiogenic agents and PARP inhibitors in platinum-sensitive recurrent ovarian cancer. *Expert Opin Drug Saf* 16:687–696.
39. Moore KN, Mirza MR, Matulonis UA (2018) The poly (ADP ribose) polymerase inhibitor niraparib: Management of toxicities. *Gynecol Oncol* 149:214–220.
40. Pujade-Lauraine E, et al. (2014) Bevacizumab combined with chemotherapy for platinum-resistant recurrent ovarian cancer: The AURELIA open-label randomized phase III trial. *J Clin Oncol* 32:1302–1308.
41. Aghajanian C, et al. (2015) Final overall survival and safety analysis of OCEANS, a phase 3 trial of chemotherapy with or without bevacizumab in patients with platinum-sensitive recurrent ovarian cancer. *Gynecol Oncol* 139:10–16.
42. Coleman RL, et al. (2017) Bevacizumab and paclitaxel-carboplatin chemotherapy and secondary cytoreduction in recurrent, platinum-sensitive ovarian cancer (NRG oncology/gynecologic oncology group study GOG-0213): A multicentre, open-label, randomised, phase 3 trial. *Lancet Oncol* 18:779–791.
43. Michel MC, Foster C, Brunner HR, Liu L (2013) A systematic comparison of the properties of clinically used angiotensin II type 1 receptor antagonists. *Pharmacol Rev* 65:809–848.
44. Ahmed N, Stenvers KL (2013) Getting to know ovarian cancer ascites: Opportunities for targeted therapy-based translational research. *Front Oncol* 3:256–268.
45. Eskander RN, Tewari KS (2012) Emerging treatment options for management of malignant ascites in patients with ovarian cancer. *Int J Womens Health* 4:395–404.
46. Zebrowski BK, et al. (1999) Markedly elevated levels of vascular endothelial growth factor in malignant ascites. *Ann Surg Oncol* 6:373–378.
47. Pinter M, Kwanten WJ, Jain RK (2018) Renin-angiotensin system inhibitors to mitigate cancer treatment-related adverse events. *Clin Cancer Res* 24:3803–3812.
48. Garber K (2009) Companies waver in efforts to target transforming growth factor beta in cancer. *J Natl Cancer Inst* 101:1664–1667.
49. Anderton MJ, et al. (2011) Induction of heart valve lesions by small-molecule ALK5 inhibitors. *Toxicol Pathol* 39:916–924.
50. Hong S, Lee HJ, Kim SJ, Hahm KB (2010) Connection between inflammation and carcinogenesis in gastrointestinal tract: Focus on TGF-beta signaling. *World J Gastroenterol* 16:2080–2093.
51. de Gramont A, Faivre S, Raymond E (2016) Novel TGF-β inhibitors ready for prime time in onco-immunology. *OncoImmunology* 6:e1257453.
52. Gueorguieva I, et al. (2014) Defining a therapeutic window for the novel TGF-β inhibitor LY2157299 monohydrate based on a pharmacokinetic/pharmacodynamic model. *Br J Clin Pharmacol* 77:796–807.
53. PharmacyChecker (2018) Available at https://www.pharmacychecker.com/losartan/.
54. Liu H, et al. (2017) Use of angiotensin system inhibitors is associated with immune activation and longer survival in nonmetastatic pancreatic ductal adenocarcinoma. *Clin Cancer Res* 23:5959–5969.
55. Cushing L, et al. (2011) miR-29 is a major regulator of genes associated with pulmonary fibrosis. *Am J Respir Cell Mol Biol* 45:287–294.
56. Castoldi G, et al. (2012) MiR-133a regulates collagen 1A1: Potential role of miR-133a in myocardial fibrosis in angiotensin II-dependent hypertension. *J Cell Physiol* 227:850–856.
57. Chen S, et al. (2014) Cardiac miR-133a overexpression prevents early cardiac fibrosis in diabetes. *J Cell Mol Med* 18:415–421.
58. Roderburg C, et al. (2013) miR-133a mediates TGF-β-dependent derepression of collagen synthesis in hepatic stellate cells during liver fibrosis. *J Hepatol* 58:736–742.
59. Satoh M, et al. (2001) Renal interstitial fibrosis is reduced in angiotensin II type 1a receptor-deficient mice. *J Am Soc Nephrol* 12:317–325.
60. Harada K, Sugaya T, Murakami K, Yazaki Y, Komuro I (1999) Angiotensin II type 1A receptor knockout mice display less left ventricular remodeling and improved survival after myocardial infarction. *Circulation* 100:2093–2099.
61. Yang L, et al. (2005) Attenuated hepatic inflammation and fibrosis in angiotensin type 1a receptor deficient mice. *J Hepatol* 43:317–323.
62. Schena FP, Serino G, Sallustio F (2014) MicroRNAs in kidney diseases: New promising biomarkers for diagnosis and monitoring. *Nephrol Dial Transplant* 29:755–763.
63. Jeffrey SS (2008) Cancer biomarker profiling with microRNAs. *Nat Biotechnol* 26: 400–401.
64. Seror O, et al. (2016) Hepatocellular carcinoma within milan criteria: No-touch multibipolar radiofrequency ablation for treatment-long-term results. *Radiology* 280: 611–621.
65. Hayes CN, Chayama K (2016) MicroRNAs as biomarkers for liver disease and hepatocellular carcinoma. *Int J Mol Sci* 17:280–297.